Supplementary Information

Fluidic Switching in Nanochannels for Control of Inchworm: A Synthetic Molecular Motor with a Power-Stroke

*Cassandra S. Niman, Martin J. Zuckermann, Martina Balaz, Jonas O. Tegenfeldt, Paul M. G. Curmi, Nancy R. Forde, Heiner Linke**

S1. The Langevin Simulation Method

The Langevin method used to simulate the motion of the IW motor is formally identical to that used by Kuwada *e*t al.[1]. Let $\Delta x_i^{(j)}$ be the change in the value of the *i*th coordinate of the *j*th monomer of the polymer over an incremental time, Δt, at time t. Here i (=1 to 3) are 3D coordinate indices and j= 1,2,…,N are the monomer indices for the polymer. The Langevin equation can then be written:

$$\Delta x_i^{(j)} = \frac{F_i^{(j)} \Delta t}{\gamma} + \left(\frac{2 k_B T \Delta t}{\gamma} \right)^{\frac{1}{2}} \zeta_i^{(j)}(t) \qquad \text{(S1)}$$

In equation (S1), $F_i^{(j)}$ is the *i*th component of the sum of both internal and external conservative forces on the *j*th monomer at time t. The value for the drag coefficient for each monomer, γ, is given by

$$\gamma = \frac{k_B T}{D} \qquad \text{(S2)}$$

Here D is the monomeric diffusion constant estimated to be $D = 3.3 \times 10^{-11}$ m^2 s^{-1} [23].
$\zeta_i^{(j)}$ is a random number taken from a Gaussian distribution with zero mean and variance $\langle \zeta_i^{(j)}(t)\ \zeta_i^{(j')}(t') \rangle = \delta_{ii'} \delta_{jj'}\, \delta(t - t')$. $F_i^{(j)}$ is the sum of a conservative force and an external force, F_M, and is given by:

$$F_i^{(j)} = F_{Ci}^{(j)} + F_M \delta_{i1} \qquad \text{(S3)}$$

Here j=1 is the direction of the axis of the cylindrical nano-channel.

The conservative force, $F_{Ci}^{(j)}$, acts on each monomer and is the negative gradient of the following potential:

$$V = W_H + W_{SB} + W_{LJ} + W_{BE} \qquad \text{(S4)}$$

W_H is a harmonic potential, which fixes the length of the bonds between the monomers of the polymer and is given by:

$$W_H = \frac{V_H}{2} \sum_{j=1,N-1} \left(\left| r_{j+1} - r_j \right| - l_B \right)^2 \qquad \text{(S5)}$$

Here $\boldsymbol{r}_j$ is the position vector for monomer j (j = 1 to N) and l_B is the bond length. The specific binding potential, W_{SB}, for binding of a DNA recognition sequence monomer to a repressor protein on the nanochannel wall is given by:

$$W_{SB}(r_j) = \begin{Bmatrix} -V_{SB}\,\mathrm{Exp}\left[-\left(\frac{r_j}{\eta}\right)^2\right]; & r_j < \eta \\ -V_{SB}\,\mathrm{Exp}[1]; & r_j \geq \eta \end{Bmatrix} \qquad \text{(S6)}$$

Here V_{SB} is the coupling constant of the specific binding interaction, η is its effective range and r_j is the distance between repressor j and the nearest corresponding dsDNA recognition sequence on the track.

The excluded volume between two distant monomers is simulated by a repulsive Lennard-Jones (LJ) interaction, W_{LJ}, given by:

$$W_{LJ}(r_{ij}) = \begin{Bmatrix} V_{LJ}\left[\left(\frac{\sigma}{r_{ij}}\right)^{12} - \left(\frac{\sigma}{r_{ij}}\right)^{6}\right] & r_{ij} < 2^{\frac{1}{6}}\sigma \\ -\frac{V_{LJ}}{4} & r_{ij} \geq 2^{\frac{1}{6}}\sigma \end{Bmatrix} \qquad \text{(S7)}$$

Here V_{LJ} is the strength of the LJ interaction, σ is the minimum distance between the centers of two spherical monomers and r_{ij} is the actual distance between them. W_{BE} is the above-mentioned bending energy potential given by:

$$W_{BE} = V_{\Theta}\sum_{j=1,N-1}\left[\cos\theta_{j,j+1} - \cos\theta_0\right]^2 \qquad \text{(S8)}$$

Here $\theta_{j,j+1}$ is the angle between the jth and j+1th polymer bonds (j=1,…,N-1) and θ_0 is taken to be π. The value of V_Θ then controls the elongation of the polymer in the nanochannel. The value of the effective range, η, of the specific binding potential of equation (S6) was taken to be 3.45 nm and the value of the lattice constant, b_R, for the square lattice of repressors used in the simulations was 8 nm. Other parameter values are given in Table S 1.

The dimensionless Langevin equation used in the simulations is written as follows:

$$\Delta\xi_j^{(j)} = \Phi_i^{(j)}\Delta\tau + \left(2\Delta\tau\right)^{\frac{1}{2}}\zeta_i^{(j)}(\tau) \quad . \qquad \text{(S9)}$$

Here ξ, τ and Φ are the dimensionless monomer coordinates, dimensionless force and dimensionless time, respectively, and are given by:

$$\xi = \frac{x}{x_0}; \quad \tau = \frac{t}{t_0}; \quad \Phi = \frac{F}{F_0} \qquad \text{(S10)}$$

The scaling quantities t_0 and F_0 are given by:

$$t_0 = \frac{\gamma x_0^{\,2}}{k_B T}; \quad F_0 = \frac{k_B T}{x_0} \tag{S11}$$

In our simulations, x_0= 50 nm and from equation (S11) and Table S1, the values for t_0 and F_0 used in our simulations are t_0 = 0.287 ms and F_0 = 0.082 pN.

Table S 1

	Symbol	Value
Temperature	$k_B T$	4.1 pN nm
Drag Coefficient	γ	$1.3\text{x}10^{-10}$ kg s^{-1}
Polymer Bond Length	l_B	100 nm
Number of monomers	N	81
Harmonic Bond Potential Coupling Constant	V_H	1.025 pJ nm^2
Lennard-Jones Distance	σ	100 nm
Lennard-Jones Interaction	V_{LJ}	16.4 pN nm
Lattice Constant	b_R	8 nm
Binding Site Density	ρ	7800 μm^{-2}
Specific Binding Interaction	V_{SB}	$8.2\text{x}10^2$ pN nm
Effective Range of the Specific Binding Interaction	η	3.45 nm
Elongation Bending Energy	V_Θ	82 pN nm
Langevin Dynamics Time Step	Δt	0.388 ns

The reasons for the choice of some of the parameter values in Table S1 are as follows:

(a) The bond length of the polymer, l_B, is essentially the Kuhn length of dsDNA and is given by twice the related persistence length (50 nm at high salt).

(b) The coupling constant of the Harmonic Bond Potential, V_H, was chosen to be sufficiently large to ensure that the bond length is practically constant.

(c) The Lennard-Jones distance, σ, defines the excluded volume of the monomers and the value used is the same as in the polymer model for dsDNA of [2].The chosen value for σ makes the polymer chain into a self-avoiding walk (SAW) as it prevents the chain from self-interacting.

(d) The coupling constant of the Lennard-Jones interaction, V_{LJ}, has the standard value of $4k_B T$ used in polymer simulations (see [2]).

(h) The time step, Δt, was chosen to be small enough to ensure that the simulation results were independent of its value.

(e) The choice of 8 nm for the lattice constant of the square lattice of binding sites on the cylindrical nanochannel wall, b_R, gives a binding site density of 15,575 μm^{-2}. The lattice is then randomly filled with 49.92% vacancies and 50.08% binding sites which are evenly and randomly distributed between A and B repressors respectively. This gives a density, ρ, of 7,800 μm^{-2}, which is the estimate for the maximum achievable experimental repressor density based on the typical physical dimensions of proteins.

(f) The coupling constant for the specific binding interaction, V_{SB}, was chosen to be large enough to achieve binding of the end monomers of the polymer to the binding sites on the nanochannel walls that was sufficiently strong so as not to break due to thermal fluctuations in the simulations.

(g) The effective range of the specific binding interaction, η, was chosen to be 3.45 nm which is less than half of the repressor lattice constant. The binding sites therefore do not overlap and a given repressor can only bind to one binding site at a time.
(h) The elongation bending energy, V_{Θ}, was chosen to be large enough to reach the lower values of the experimentally applied ionic strength for dsDNA (see main text).

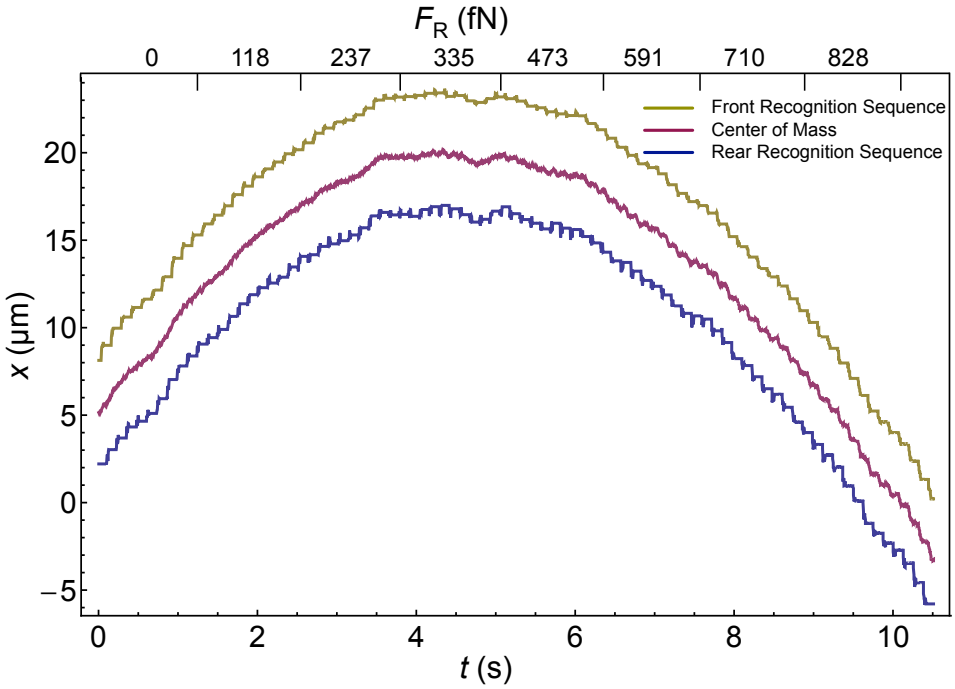

Figure S1. Brownian dynamics simulations results. Position, x, of the front (Yellow), Center (Pink), and Rear (Blue) of the DNA vs. time where rearward force is incrementally increasing by steps of 118 fN every 1.3 s. This shows the continuous data for the rearward force simulations, also shown in Figure 2D.

S2. IW Stall Force Predicted from DNA Spring Constant

Our modeling results indicate that IW stalling occurs as a consequence of competition between salt-induced contraction and extension of the DNA, and the counteracting extension and compression due to a load force, in States II and IV, respectively. Based on this consideration, we estimate IW's stall force from IW's spring constant (which counteracts load-force induced extension and compression).

We thus assume that stalling occurs in the model when the rearward force is sufficiently large to induce a length change ΔL equal to that induced by salt changes.

In the model, the total rearward force F is the sum of all forces applied to each monomer. To calculate the resulting extension we integrate over the DNA's extensions due to each partial force $(F/L)dl$ applied to each segment dl, where we take l to be the coordinate along the contour of the polymer.

Knowing that the spring constant of a polymer is inversely proportional to the total length [4], we can find the effective spring constant as a function of the force's attachment point l as

$$\kappa_l = \kappa \frac{L}{l}, \tag{S12}$$

where κ is the spring constant of the entire polymer. Using Hooke's law we can then write the total change in length as

$$\Delta L = \int_0^L \frac{F}{L} \frac{1}{\kappa_l} dl = \int_0^L \frac{F}{L} \frac{l}{\kappa \cdot L} dl = \frac{F}{2\kappa} \tag{S13}$$

Stalling occurs when $F = F_{\text{stall}}$ is sufficiently large such that the resulting ΔL equals that induced by salt changes (0.7 μm in our model). Thus, based on these considerations, we predict $F_{\text{stall}} = 2\kappa\Delta L = 0.23$ pN for $\Delta L = 0.7$ μm and $\kappa = 0.16$ pN μm^{-1}.

S3. Calculating Switching Times

We define switching times, t_s, from the raw data sets of intensity vs. time (example shown in Figure 5 of the main text) as the time to go from 80% to 20% of the fluorescence intensity measured. To determine t_s we used seven switching events, and in each dataset we used a moving average of seven data points to reduce noise, rounding the relative intensity values to the nearest 0.001.

S4. Analytical Expression Derivation

When the pressure across the nanochannels is zero, in force-free mode, we find the concentration profile by solving Fick's law,

$$\frac{\partial C\left(x_{\text{NC}},t\right)}{\partial t} = D \frac{\partial^2 C\left(x_{\text{NC}},t\right)}{\partial {x_{\text{NC}}}^2}, \tag{S14}$$

with the following boundary conditions, initial condition and equilibrium condition:

Boundary Conditions: $C\left(x_{\text{NC}}=0,t\right)=1$

$C\left(x_{\text{NC}}=l,t\right)=0$,

Initial Condition: $C\left(x_{\text{NC}},t=0\right)=0$,

Equilibrium Condition: $C\left(x_{\text{NC}},t=\infty\right)=C_{\text{eq}}\left(x_{\text{NC}}\right)=\left(1-\frac{x_{\text{NC}}}{l}\right)$.

The equilibrium profile is shown in Figure 7. We define the concentrations as the sum of the final concentration profile and a perturbation from equilibrium, ΔC,

$$C\left(x_{\text{NC}},t\right) = C_{\text{eq}}\left(x_{\text{NC}}\right) + \Delta C\left(x_{\text{NC}},t\right) \tag{S15}$$

and substitute equation (S15) into equation (S14)

$$\frac{\partial}{\partial t}\Delta C\left(x_{\text{NC}},t\right) = D \frac{\partial^2}{\partial {x_{\text{NC}}}^2}\Delta C\left(x_{\text{NC}},t\right) \tag{S16}$$

Then solve for ΔC dependence on position and time

$$\Delta C\left(x_{\mathrm{NC}},t\right)=\sum_{n=1}^{\infty}A_n Exp\left[\lambda_n t\right]\sin\left[\frac{n\pi x_{\mathrm{NC}}}{l}\right]\quad;\quad\lambda_n=-D\left(\frac{n\pi}{l}\right)^2$$

$$\Delta C\left(x_{\mathrm{NC}},t=0\right)=\left(\frac{x_{\mathrm{NC}}}{l}-1\right)=\sum_{n=1}^{\infty}A_n\sin\left[\frac{n\pi x_{\mathrm{NC}}}{l}\right]$$

$$A_n=\frac{2}{l}\int_0^l\left(\frac{x_{\mathrm{NC}}}{l}-1\right)\sin\left[\frac{n\pi x_{\mathrm{NC}}}{l}\right]dx_{\mathrm{NC}}=-\frac{2}{n\pi}$$

We use this result to find the final concentration dependence on position and time

$$C\left(x_{\mathrm{NC}},t\right)=1-\left\{\frac{x_{\mathrm{NC}}}{l}+\frac{2}{\pi}\sum_{n=1}^{\infty}\frac{1}{n}\mathrm{Exp}\left[-Dt\left(\frac{n\pi}{l}\right)^2\right]\sin\left[\frac{n\pi x_{\mathrm{NC}}}{l}\right]\right\}\qquad\text{(S17)}$$

The concentration profile when there is a pressure drop across the nanochannels, in constant-force mode, was found in [5] to be

$$C\left(x_{\mathrm{NC}},t\right)=1-\mathrm{Erf}\left[\frac{x_{\mathrm{NC}}-vt}{2\sqrt{D_{\mathrm{eff}}t}}\right]\qquad\text{(S18)}$$

S5. Microfluidic simulations

The COMSOL multiphysics simulation of the full microfluidics used experimentally matches well with experimentally obervations[6] The concentration of the fluid shown in the close-up view of the center channel micifluidics in Figure S2A matches well with the experimental observations shown in Figure 5D. The pressure of the fluid in the region of the microfluidics channels connected to the nanochannels is shown in Figure S2B, cooresponding to force-free mode (top) and constant-force mode (bottom) used experimentally.

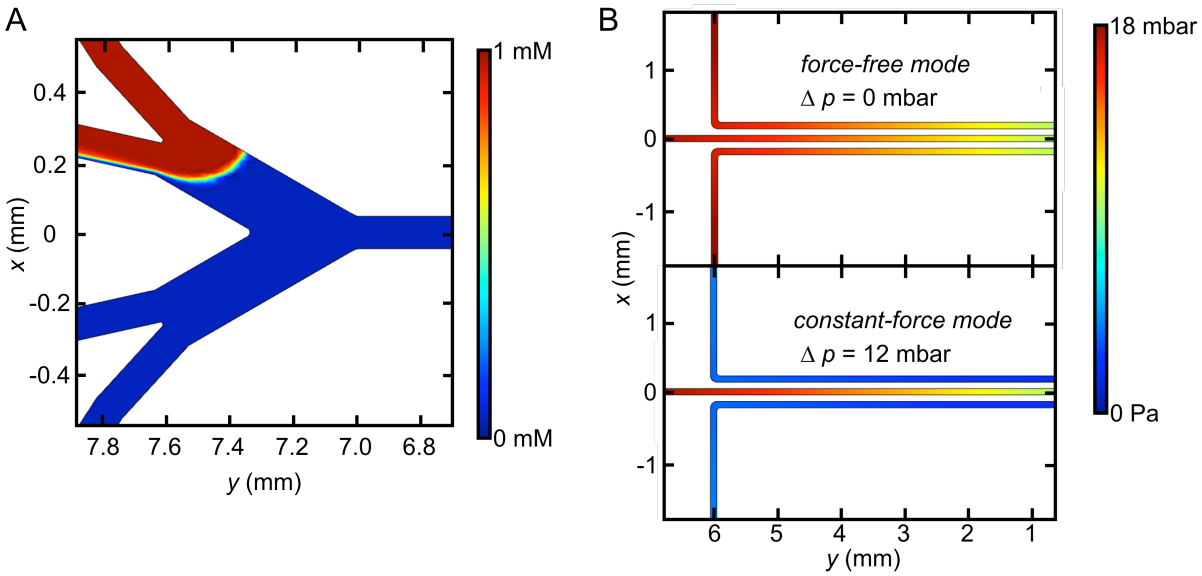

Figure S2. (A) Concentration of the fluid in the center channel for the simulated microfluidics using experimentally used pressure values. This matches the observed fluorescence in Figure 5D. (B) The simulated pressure gradient in the center and side microfluidic channels in the region the nanochannels are aligned experimentally, for the force-free mode (top) and the constant-force mode (bottom) using experimental inlet pressures. In constant-force mode the pressure drop across the nanochannels is found to be 12 mbar.[6]

To investigate the fluid dynamics in the nanochannels just below the center microfluidics channel, where the fluid switching is fastest and could not be examined experimentally we have simulated a cross section including seven nanochannels connected to a large microchannel above. In Figure S3 we can see the velocity profile in the microchannel when there is a pressure drop of 0.26 mbar, as determined from the previouse simulations, with fluid coming in from the left. It is clear that although there is a relativly high fluid velocity in the microchannel the fluid velcoity in the nanochannels is negligable, at ~10^{-15} m s^{-1}.

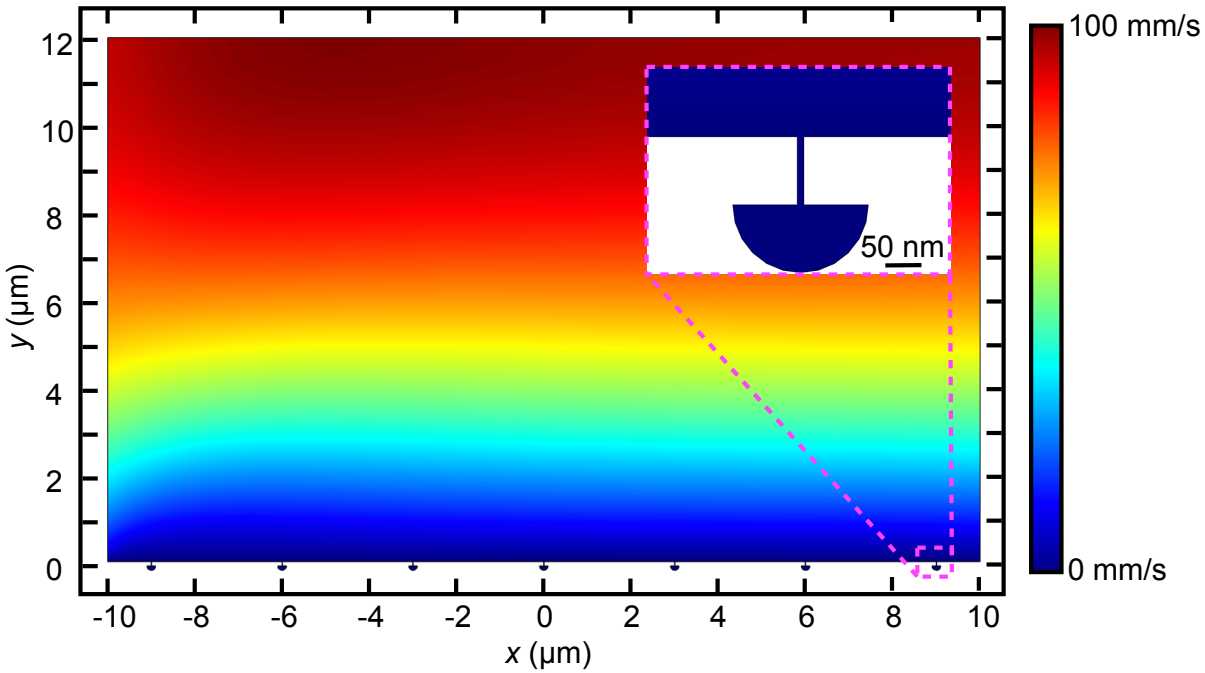

Figure S3. Cross section of the simulated fluid velocity in the center microfluidic channel with seven nanochannels perpendicularly connected below via a topslit. The color gradient is the speed of the fluid moving from left to right in the upper channel. The inset shows the low fluid speed in the last nanochannel.[6]

In the same silumation we also use a time-dependent solution to investigate the time for the solute in the upper channel to reach the nanochannels. With an initial fluid cencentration in the channels of 0 mM, and an input of the left of 1 mM at t = 0 s we observe a compete filling of the nanochannel via diffusion through the top slit in less than 5 ms. In the analysis of the experiments we consider this to be negligable when compared to the switching times in the nanochannels measured 62.5 µm from the center channel on the order of seconds. Figure S4 shows the results of this simulation at t = 0 s, 1 ms and 2 ms, with a closeup of the nanochannel furthest from the inelt.

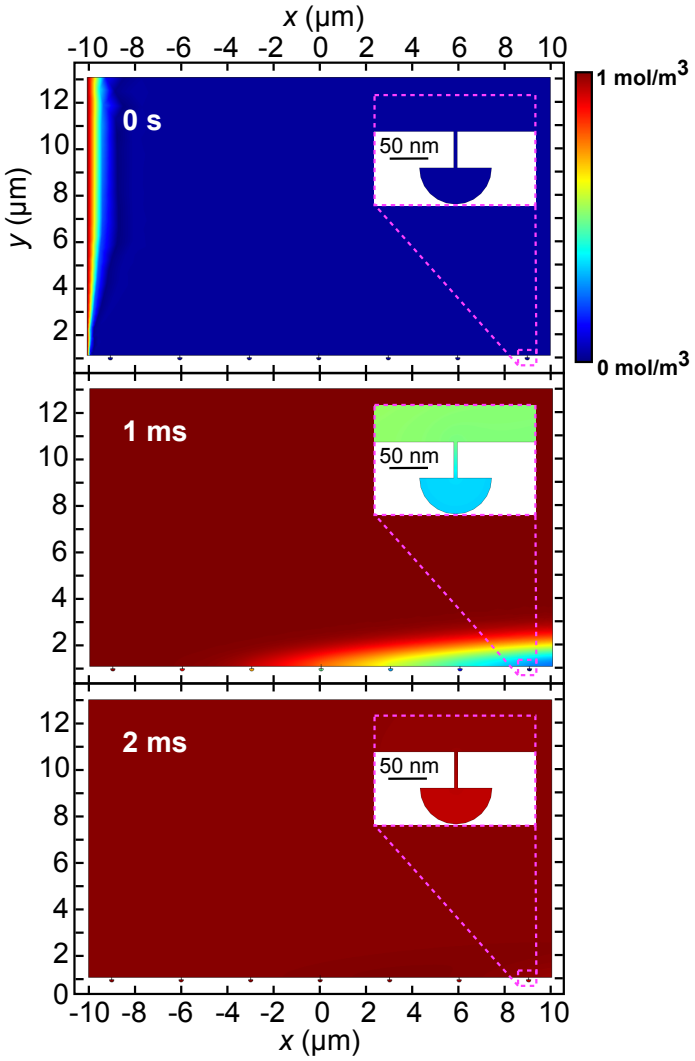

Figure S4. A cross section of the fluid concentration at three sequential times; 0 ms, 1 ms, and 2 ms; in a simulation of fluid moving through the upper microfluidic channel from left to right with seven nanochannels connected below. The solute exchange via diffusion into the last nanochannel is shown in the insets.[6]

1. N. J. Kuwada, M. J. Zuckermann, E. H. C. Bromley, R. B. Sessions, P. M. G. Curmi, N. R. Forde, D. N. Woolfson, and H. Linke, *Phys. Rev. E*, 2011, 84.
2. M. T. Downton, M. J. Zuckermann, E. M. Craig, M. Plischke, and H. Linke, *Phys. Rev. E - Stat. Nonlinear, Soft Matter Phys.*, 2006, **73**.
3. M. Liu and J. Giddings, *Macromolecules*, 1993, 3576–3588.
4. W. Reisner, J. N. Pedersen, and R. H. Austin, *Reports Prog. Phys.*, 2012, 75, 106601.
5. H. Bruus, *Physics (College. Park. Md).*, 2008, **18**, 363.
6. 2012, Version 4.3a.